Advances in structure-based turbulence modeling

By S. C. Kassinos AND W. C. Reynolds

1. Motivation and objectives

Turbulent flows of importance in aircraft and propulsion system design involve complex three-dimensional time-dependent mean flow, where the turbulence is often subjected to very rapid deformation and strong mean rotation or curvature effects. In these flows the structure of the turbulence plays an important role in determining the transport of the Reynolds stresses, and because the turbulence structure takes some time to respond to the imposed deformation, an eddy-viscosity representation is not appropriate. The ability of aerospace engineers to predict these complex flows is limited by the current state-of-the-art in one-point turbulence modeling, which invariably relies on an eddy-viscosity approach.

The response of turbulence to the kind of deformation that is often encountered in engineering applications (rapid rates and/or strong rotation) is described well by Rapid Distortion Theory (RDT). RDT is a closed two-point theory, but engineering models require one-point formulation. Therefore, what is needed is a one-point model that matches eddy viscosity models for weak deformation rates and RDT for rapid deformations.

The weakness of standard models is due to incomplete information and is particularly troublesome in flows with strong mean rotation. We have shown that it is impossible to model the effects of strong mean rotation or curvature using only the information found in the turbulent stresses themselves. The critical information that must be added relates to the dimensionality of the turbulence structure (see Kassinos & Reynolds 1994). We have introduced a number of one-point turbulent structure tensors that carry this additional information and have derived their exact transport equations (Kassinos & Reynolds 1994). These tensors include the second-rank structure *dimensionality* D_{ij} and structure *circulicity* F_{ij}, and the third-rank, fully symmetric, structure *stropholysis* Q^*_{ijk}. A detailed account of the role of these tensors is given in Kassinos & Reynolds (1994) and Reynolds & Kassinos (1995).

We have completed the formulation of a successful particle representation model (Kassinos and Reynolds 1996) which has the correct viscoelastic character. This model, which we have termed the Interacting Particle Representation Model (IPRM), is a non-local method that can handle remarkably well almost any mean deformation of homogeneous turbulence. The IPRM is exact in the limit of RDT, which it matches with no modeling. With relatively simple structure-based modeling of the non-linear interactions, the IPRM is able to match eddy-viscosity theory for weak deformations and to provide a reasonable blend between eddy-viscosity and RDT for conditions that fall between the two limits. More details on the IPRM formulation are given in Kassinos & Reynolds (1996).

The IPRM is a non-local model, but for engineering use we need one-point formulation. More recently our efforts have been focused on the development of a

one-point structure-based model using the IPRM as the starting point. The present study outlines the formulation for these more recent developments and gives representative results where appropriate. An in-depth discussion of the IPRM and the corresponding one-point model is given in a separate manuscript under preparation.

2. Accomplishments

In Section 2.1 we introduce notation and review the basic formulation of the IPRM. Then in Section 2.2, we present the formulation of a one-point model that follows directly from the IPRM. The IPRM emulates RDT exactly because the non-local rapid pressure fluctuations can be evaluated exactly. This is not the case for the one-point model, which requires additional modeling to deal with the non-locality of the pressure fluctuations. Section 2.2 includes a discussion of this additional modeling. In Section 2.3 we evaluate the one-point model for a number of representative flows.

2.1 An Interacting Particle Representation Model (IPRM)

In a particle representation method, a number of key properties and their evolution equations are assigned to hypothetical particles. The idea is to follow an ensemble of "particles", determine the statistics of the ensemble, and use those as the representation for the one-point statistics of the corresponding field. It is important to appreciate that these particles do not have to be physical elements of fluid. The idea of representing the turbulent flow by a large number of particles, each having its own set of properties, has been used over the past ten years by the combustion community in the form of Lagrangian PDF methods (for example see Pope 1994). In these traditional approaches a stochastic model is used, which can be chosen so that upon taking moments of the governing stochastic evolution equations one recovers one of the standard Reynolds stress transport (RST) models. This approach, however, uses modeling where it is not required, *i.e.* in emulating RDT. A more detailed discussion of the rapid PRM can be found in Kassinos & Reynolds (1994); Vanslooten & Pope (1997) have recently used the ideas given there to construct a PDF model that is consistent with RDT.

2.1.1 Particle properties

We start with a discussion of the properties assigned to each of the hypothetical particles. The assigned properties are:

- **V** velocity vector
- **W** vorticity vector
- **S** stream function vector
- **N** gradient vector
- P pressure.

Here we consider a representation method using non-physical "particles" that correspond most closely to a vortex sheet (or 1D-1C flow). The only axis of dependence lies normal to the vortex sheet and parallel to the N_i vector, which provides a measure of gradients normal to the plane. The remaining vectors lie in the plane of independence.

2.1.2 Representations for one-point statistics

The Reynolds stress $R_{ij} = \overline{u_i' u_j'}$ is represented as

$$R_{ij} = \langle V_i V_j \rangle = \langle V^2 v_i v_j \rangle \,, \tag{1}$$

where the angle brackets denote averaging over an ensemble of particles and $v_i = V_i/\sqrt{V_k V_k}$. Two one-point turbulent tensors that carry useful structure information are the structure *dimensionality* and *circulicity*, defined by

$$D_{ij} = \overline{\Psi'_{n,i} \Psi'_{n,j}} \qquad F_{ij} = \overline{\Psi'_{i,n} \Psi'_{j,n}} \,. \tag{2}$$

Here Ψ_i' is the turbulent stream function vector, which satisfies

$$u_i' = \epsilon_{its} \Psi'_{s,t} \qquad \Psi'_{i,i} = 0 \qquad \Psi'_{i,nn} = -\omega_i' \tag{3}$$

and ω_i' is the fluctuation vorticity. In the IPRM formulation the structure tensors are represented as

$$D_{ij} = \langle S_n S_n N_i N_j \rangle = \langle V^2 n_i n_j \rangle \tag{4}$$

$$F_{ij} = \langle N_n N_n S_i S_j \rangle = \langle V^2 s_i s_j \rangle \tag{5}$$

where $n_i = N_i/\sqrt{N_k N_k}$ and $s_i = S_i/\sqrt{S_k S_k}$. A consequence of the orthogonality of the three vectors n_i, v_i, and s_i is that, for homogeneous turbulence, the three second-rank tensors satisfy the constitutive equation

$$R_{ij} + D_{ij} + F_{ij} = q^2 \delta_{ij} \,. \tag{6}$$

Here $q^2 = 2k = R_{ii}$. For homogeneous turbulence $D_{ii} = F_{ii} = q^2$, and it is possible to normalize (6) so that

$$r_{ij} + d_{ij} + f_{ij} = \delta_{ij} \tag{7}$$

where

$$r_{ij} = R_{ij}/q^2 \qquad d_{ij} = D_{ij}/q^2 \qquad f_{ij} = F_{ij}/q^2 . \tag{8}$$

The tensor anisotropies $\tilde{r}_{ij} = r_{ij} - \frac{1}{3}\delta_{ij}$, $\tilde{d}_{ij} = d_{ij} - \frac{1}{3}\delta_{ij}$, and $\tilde{f}_{ij} = f_{ij} - \frac{1}{3}\delta_{ij}$ satisfy

$$\tilde{r}_{ij} + \tilde{d}_{ij} + \tilde{f}_{ij} = 0 \,. \tag{9}$$

In the inhomogeneous case additional terms appear in (6) and (9) (see Kassinos & Reynolds 1994).

2.2.3 Emulation of the Rapid Distortion Theory

The evolution of the vector properties assigned to each particle are governed by ordinary differential equations based on the Navier-Stokes equations. For example, a kinematic analysis leads to the RDT evolution equation for **N**

$$\dot{N}_i = -G_{ki} N_k \,, \tag{10}$$

which shows that $\mathbf{N}$ plays a role similar to that of the wavenumber vector $\mathbf{k}$. Here $G_{ij} = U_{i,j}$ is the mean velocity gradient tensor. The unit vector $n_i = N_i/\sqrt{N_k N_k}$ satisfies

$$\dot{n}_i = -G_{ki} n_k + G_{km} n_k n_m n_i \,. \tag{11}$$

The PRM evolution equation for $\mathbf{V}$ is

$$\dot{V}_i = -G_{ik} V_k + 2 G_{km} \frac{V_m N_k N_i}{N^2}. \tag{12}$$

The familiar Poisson equation for the rapid pressure is the basis for the analogous definition

$$P = -2 G_{km} \frac{V_m N_k}{N^2} \,. \tag{13}$$

Using (12) and (13), one obtains

$$\dot{V}_i = -G_{ik} V_k - P N_i \tag{14}$$

by analogy to the fluctuation momentum equation under RDT.

2.1.4 Cluster-averaged equations

The cluster-averaged implementation of the PRM offers a better computational efficiency. The idea is to do the averaging in two steps, the first step being done analytically. First, an averaging is done over particles that have the same $\mathbf{n}(t)$, followed by an averaging over all particles with different $\mathbf{n}(t)$. The one-point statistics resulting from the first (cluster) averaging are conditional moments, which will be denoted by

$$R_{ij}^{|\mathbf{n}} \equiv \langle V_i V_j | \mathbf{n} \rangle \qquad D_{ij}^{|\mathbf{n}} \equiv \langle V^2 n_i n_j | \mathbf{n} \rangle = \langle V^2 | \mathbf{n} \rangle n_i n_j$$

and

$$F_{ij}^{|\mathbf{n}} \equiv \langle V^2 s_i s_j | \mathbf{n} \rangle. \tag{15}$$

The conditionally-averaged stress evolution equation

$$\dot{R}_{ij}^{|\mathbf{n}} = -G_{ik} R_{kj}^{|\mathbf{n}} - G_{jk} R_{ki}^{|\mathbf{n}} + 2 G_{km} (R_{im}^{|\mathbf{n}} n_k n_j + R_{jm}^{|\mathbf{n}} n_k n_i) \tag{16}$$

is obtained by using the definition (15) along with (12). Note that (11) and (16) are *closed* for the conditional stress tensor $R_{ij}^{|\mathbf{n}}$ and n_i. That is, they can be solved without reference to the other conditioned moments.

2.1.5 Formulation of the nonlinear model

Whenever the time scale of the mean deformation is large compared to that of the turbulence, the nonlinear turbulence-turbulence interactions become important in the governing field equations. In the context of the Interacting Particle Representation Model (IPRM), these nonlinear processes are represented by a model for the particle-particle interactions.

Direct numerical simulations (Lee & Reynolds 1985) show that under weak strain the structure dimensionality D_{ij} remains considerably more isotropic than does the Reynolds stress R_{ij}. This leads to counter-intuitive R_{ij} behavior in axisymmetric expansion flows (see Section 2.3.1), supported by experiments (Choi 1983). Hence we modify the basic evolution equations (11) and (16) to account for these effects. The resulting cluster-averaged evolution equations are

$$\dot{n}_i = -G^n_{ki} n_k + G^n_{kr} n_k n_r n_i \tag{17}$$

$$\begin{aligned} \dot{R}^{|\mathbf{n}}_{ij} = & -G^v_{ik} R^{|\mathbf{n}}_{kj} - G^v_{jk} R^{|\mathbf{n}}_{ki} - C_r[2R^{|\mathbf{n}}_{ij} - R^{|\mathbf{n}}_{kk}(\delta_{ij} - n_i n_j)] \\ & + [G^n_{km} + G^v_{km}](R^{|\mathbf{n}}_{im} n_k n_j + R^{|\mathbf{n}}_{jm} n_k n_i)\,. \end{aligned} \tag{18}$$

Note that the mean velocity gradient tensor G_{ij} that appeared in (11) and (16) has been replaced by the *effective* gradient tensors G^v_{ij} and G^n_{ij}. These are defined by

$$G^n_{ij} = G_{ij} + \frac{C_n}{\tau} r_{ik} d_{kj} \qquad G^v_{ij} = G_{ij} + \frac{C_v}{\tau} r_{ik} d_{kj}\,. \tag{19}$$

Here $r_{ij} = R_{ij}/q^2$ and $d_{ij} = D_{ij}/q^2$ where $q^2 = 2k = R_{ii}$. The two constants are taken to be $C_n = 2.2 C_v = 2.2$. The different values for these two constants account for the different rates of return to isotropy of $\mathbf{D}$ and $\mathbf{R}$. The time scale of the turbulence τ is evaluated so that the dissipation rate in the IPRM

$$\epsilon^{\mathrm{PRM}} = q^2 \frac{C^v}{\tau} r_{ik} d_{km} r_{mi} \tag{20}$$

matches that obtained from a modified model equation for the dissipation rate,

$$\dot{\epsilon} = -C_0(\epsilon^2/q^2) - C_s S_{pq} r_{pq} \epsilon - C_\Omega \sqrt{\Omega_n \Omega_m d_{nm}}\, \epsilon\,. \tag{21}$$

The last term in (21) accounts for the suppression of ϵ by mean rotation. Here Ω_i is the mean vorticity vector, and the constants are taken to be

$$C_0 = 3.67 \qquad C_s = 3.0 \qquad \text{and} \qquad C_\Omega = 0.01\,. \tag{22}$$

Mean rotation acting on the particles tends to produce rotational randomization of the $\mathbf{V}$ vectors around the $\mathbf{n}$ vectors (Mansour *et al.* 1991, Kassinos & Reynolds 1994). The third (bracketed) term on the RHS of (18), is the *slow rotational randomization model*, which assumes that the effective rotation due to nonlinear particle-particle interactions, $\Omega^*_i = \epsilon_{ipq} r_{qk} d_{kp}$, should induce a similar randomization effect while leaving the conditional energy unmodified. Based on dimensional considerations and requirements for material indifference to rotation (Speziale 1981, 1985), we take

$$C_r = \frac{8.5}{\tau}\, \Omega^*\, f_{pq} n_p n_q, \quad \Omega^* = \sqrt{\Omega^*_k \Omega^*_k}, \quad \Omega^*_i = \epsilon_{ipq} r_{qk} d_{kp}\,. \tag{23}$$

The rotational randomization coefficient C_r is sensitized to the orientation of the $\mathbf{n}$ vector so that the slow rotational randomization vanishes whenever the large-scale circulation is confined in the plane normal to $\mathbf{n}$.

The pressure P is determined by the requirement that $R_{ik}^{|\mathbf{n}} n_k = 0$ is maintained by (17) and (18). This determines the effects of the slow pressure strain–rate-term without the need for further modeling assumptions

$$P = \underbrace{-2G_{mk}\frac{V_k N_m}{N^2}}_{\text{rapid}} - \underbrace{\frac{(C^v + C^n)}{\tau} r_{mt} d_{tk} \frac{V_k N_m}{N^2}}_{\text{slow}} . \tag{24}$$

2.2 A one-point **R-D** *model*

A one-point structure-based model for the deformation of homogeneous turbulence can be derived directly from the IPRM formulation. At the one-point level, additional modeling assumptions must be introduced in order to deal with the non-locality of the pressure fluctuations. Here we restrict the formulation of the one-point model to the case of irrotational deformation of homogeneous turbulence and discuss briefly the more general case.

As a result of the constitutive equation (6), a *structure-based* one-point model must carry the transport equations for only two of the three second-rank tensors. Here we propose a model based on the R_{ij} and D_{ij} equations, which are the one-point analogs of (17) and (18). Using the definitions (1) and (2) and the evolution equations (17) and (18), and averaging over all clusters, one obtains

$$\dot{D}_{ij} = -D_{ik}G^n_{kj} - D_{jk}G^n_{ki} + 2q^2 G^n_{km} Z^d_{kmij} - 2G^v_{km} M_{mkij} \tag{25}$$

and

$$\begin{aligned} \dot{R}_{ij} = & -G^v_{ik}R_{kj} - G^v_{jk}R_{ki} \\ & - \hat{C}_r f_{pq}[2M_{ijpq} - (\delta_{ij}D_{pq} - q^2 Z^d_{ijpq})] \\ & + [G^n_{km} + G^v_{km}](M_{imkj} + M_{jmki}) . \end{aligned} \tag{26}$$

Here G^n_{ij} and G^v_{ij} are as defined for the IPRM in (19), and $\hat{C}_r = 8.5\Omega^*/\tau$ where Ω^* is given in (23). The fourth-rank tensors

$$Z^d_{ijkm} = \langle V^2 n_i n_j n_k n_m \rangle / q^2 \quad \text{and} \quad M_{ijpq} = \langle V^2 v_i v_j n_p n_q \rangle \tag{27}$$

must be modeled. Note that $\mathbf{Z}$ is the fully symmetric, energy-weighted fourth moment of a single vector, for which we have been able to construct a good model. What is more, one can use an exact decomposition based on group theory (see Kassinos & Reynolds 1994) to express M_{ijpq} in terms of fourth moments of a single vector and the second-rank tensors R_{ij} and D_{ij}:

$$\begin{aligned} M_{ipqj} = & \tfrac{1}{2}q^2(Z^f_{ipqj} - Z^r_{ipqj} - Z^d_{ipqj}) + \frac{1}{6}\big[-3\delta_{ip}\delta_{qj}q^2 \\ & + 4(\delta_{qj}R_{ip} + \delta_{ip}D_{qj}) + 2(\delta_{qj}D_{ip} + \delta_{ip}R_{qj})\big] . \end{aligned} \tag{28}$$

Note that in the presence of mean rotation (28) involves additional terms that require modeling of the *stropholysis* effects (see section 3). Here

$$Z^r_{ijpq} = \langle V^2 v_i v_j v_p v_q \rangle / q^2 \quad \text{and} \quad Z^f_{ijpq} = \langle V^2 s_i s_j s_p s_q \rangle / q^2 . \tag{29}$$

Substituting (28) in (25) and (26) and using the definitions (8), one obtains

$$\begin{aligned} \dot{d}_{ij} = & -d_{jk}G^n_{ki} - d_{ik}G^n_{kj} + 2G^v_{km}r_{km}(d_{ij} - \tfrac{2}{3}\delta_{ij}) \\ & - \tfrac{2}{3}G^v_{km}d_{mk}\delta_{ij} + G^v_{kk}(\delta_{ij} - \tfrac{4}{3}d_{ij} - \tfrac{2}{3}r_{ij}) \\ & + (2G^n_{km} + G^v_{km})Z^d_{kmij} + G^v_{km}Z^r_{mkij} - G^v_{km}Z^f_{mkij} \end{aligned} \tag{30}$$

and

$$\begin{aligned} \dot{r}_{ij} = & \tfrac{1}{3}(G^v_{mj} + G^n_{mj})(2d_{mi} + r_{mi}) \\ & + \tfrac{1}{3}(G^v_{mi} + G^n_{mi})(2d_{mj} + r_{mj}) \\ & + \tfrac{1}{3}G^v_{jm}(d_{mi} - r_{mi}) + \tfrac{1}{3}G^v_{im}(d_{mj} - r_{mj}) \\ & + \tfrac{1}{3}G^n_{jm}(d_{mi} + 2r_{mi}) + \tfrac{1}{3}G^n_{im}(d_{mj} + 2r_{mj}) \\ & + 2G^v_{km}r_{km}r_{ij} - \tfrac{1}{2}(G^v_{ij} + G^v_{ji} + G^n_{ij} + G^n_{ji}) \\ & + (G^v_{mk} + G^n_{mk})(Z^f_{ikmj} - Z^r_{ikmj} - Z^d_{ikmj}) \\ & - \hat{C}_r f_{pq}[Z^f_{ijpq} - Z^r_{ijpq} + \tfrac{2}{3}\delta_{pq}(r_{ij} - f_{ij}) \\ & + \tfrac{1}{3}\delta_{ij}(r_{pq} - f_{pq})] . \end{aligned} \tag{31}$$

Closure of (30) and (31) in the irrotational case requires a consistent model for the fully symmetric tensors Z^n_{ijpq}, Z^r_{ijpq}, and Z^f_{ijpq}. We have constructed a model for the energy-weighted fourth moment of any vector t_i in terms of its second moment t_{ij} that allows the successful closure of (30) and (31) while maintaining *full realizability*. The same model can be used for each of the three vectors v_i, n_i, and s_i and their moments and has the general form

$$\begin{aligned} Z^t_{ijpq} = & \langle V^2 t_i t_j t_p t_q \rangle / q^2 = C_1\, \mathbf{i} \circ \mathbf{i} + C_2\, \mathbf{i} \circ \mathbf{t} \\ & + C_3\, \mathbf{t} \circ \mathbf{t} + C_4\, \mathbf{i} \circ \mathbf{t^2} + C_5\, \mathbf{t} \circ \mathbf{t^2} + C_6\, \mathbf{t^2} \circ \mathbf{t^2} . \end{aligned} \tag{32}$$

Here $\mathbf{i}$ and $\mathbf{t}$ stand for δ_{ij} and $t_{ij} = \langle V^2 t_i t_j \rangle / q^2$ respectively. Extended tensor notation is used in (32), where the fully symmetric product of two second-rank tensors $\mathbf{a}$ and $\mathbf{b}$ is denoted by

$$\mathbf{a} \circ \mathbf{b} \equiv a_{ij}b_{pq} + a_{ip}b_{jq} + a_{jp}b_{iq} + a_{iq}b_{jp} + a_{jq}b_{ip} + a_{pq}b_{ij} . \tag{33}$$

The coefficients C_1-C_6 are functions of the invariants of t_{ij} and determined by enforcing the trace condition $Z^t_{ijkk} = t_{ij}$, 2D realizability conditions for the case when the vectors t_i lie in a plane, and an important identity,

$$\mathbf{Z}^a = \tfrac{1}{16}\mathbf{i} \circ \mathbf{i} - \tfrac{1}{8}\mathbf{i} \circ \mathbf{b} + \tfrac{3}{8}\mathbf{Z}^b , \tag{34}$$

which applies between the fourth moments of two vectors a_i and b_i when a_i is randomly distributed about b_i. Kassinos & Reynolds (1994) gave an earlier **Z** model that does not exactly satisfy (34). The new coefficients will be published separately.

Next, we consider the performance of the Interacting Particle Representation Model (IPRM) and the one-point **R-D** model for three cases of irrotational mean deformation.

2.3 Evaluation of the **R-D** *model for irrotational flows*

In this section, the IPRM based on (17), (28), (21), and (29) and the one-point model based on (21), (25), (26), and (32) are evaluated for several cases of irrotational deformation of homogeneous turbulence. The examples considered here show that, even with a relatively simple closure for nonlinearity, both models achieve remarkably accurate predictions. Additional examples of the IPRM performance are also given in Kassinos & Reynolds (1994) for RDT (large Sk/ϵ), and in Kassinos & Reynolds (1996) for the general deformation of homogeneous turbulence. The evaluation of the complete **R-D** model (for combinations of mean strain and mean rotation) will be given separately.

2.3.1 Irrotational axisymmetric strain

First we consider the performance of the IPRM and the **R-D** model for the case of homogeneous, initially isotropic turbulence subjected to irrotational axisymmetric mean deformation. The mean velocity gradient tensor is given by

$$S_{ij} = \begin{pmatrix} S & 0 & 0 \\ 0 & -S/2 & 0 \\ 0 & 0 & -S/2 \end{pmatrix} \tag{35}$$

with $S > 0$ for contraction (nozzle flow) and $S < 0$ for expansion (diffuser flow). In all the cases considered here, the axis of symmetry is taken to be x_1 and the evolution histories are plotted against

$$C = \exp\left(\int_0^t |S_{\max}(t')|\, dt' \right),$$

where $S_{\max}$ is the largest principal value of the mean strain tensor.

Axisymmetric Contraction

A first case of slow irrotational axisymmetric deformation of homogeneous, initially isotropic turbulence is considered in Fig. 1. The initial parameters in this axisymmetric contraction flow ($Sq_0^2/\epsilon_0 = 1.1$) correspond to the slowest run in the 1985 simulations of Lee & Reynolds. The anisotropy evolution histories for $\tilde{\mathbf{r}}$, $\tilde{\mathbf{d}}$, and $\tilde{\mathbf{f}}$ predicted by the non-local IPRM (solid lines) and the one-point **r-d** model (dashed lines) are in satisfactory agreement with simulation results (symbols). Both models predict decay of the turbulent kinetic energy k and dissipation rate ϵ at the correct rates (see Fig. 1d).

A case of rapid axisymmetric contraction flow ($Sq_0^2/\epsilon_0 = 110.0$) is shown in Fig. 2. Comparison of the models is again made with results from the simulations of Lee &

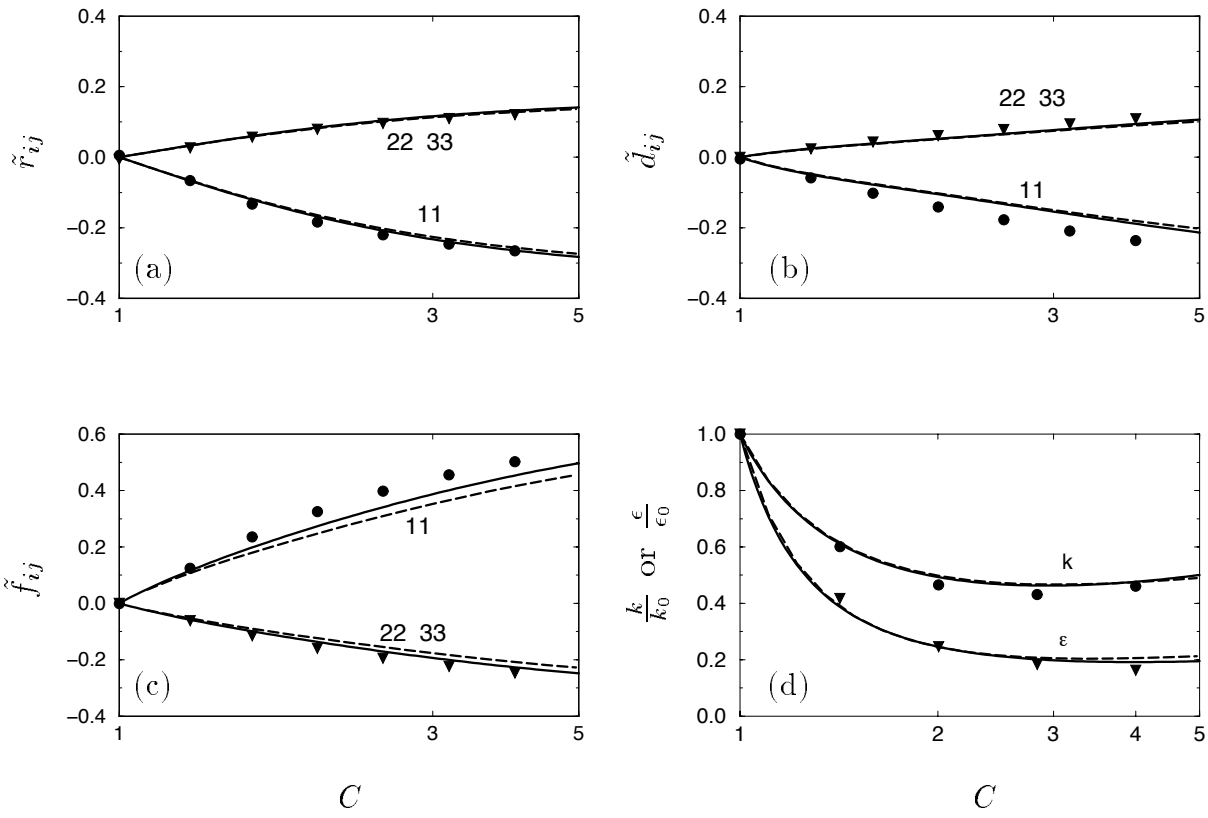

FIGURE 1. Comparison of the one-point model predictions (dashed lines) with the IPRM results (solid lines) and the 1985 DNS of Lee & Reynolds (symbols) for axisymmetric expansion case AXK ($Sq_0^2/\epsilon_0 = 1.1$). (a)-(c) evolution of the the Reynolds stress, dimensionality, and circulicity anisotropies; 11 component (•), 22 and 33 components (▼). (d) evolution of the normalized turbulent kinetic energy (•) and dissipation rate (▼).

Reynolds (shown as symbols). Note the excellent agreement of both the IPRM and the one-point model with the simulation results. Rapid Distortion Theory (RDT) predicts that under irrotational deformation $r_{ij} = d_{ij} = \frac{1}{2}(\delta_{ij} - f_{ij})$, and this result is captured by both models.

Axisymmetric Expansion

Results for the case of irrotational axisymmetric expansion flow with an initial $Sq_0^2/\epsilon_0 = 0.82$ are shown in Fig. 2. The predictions of the IPRM (solid lines) and those of the one-point model (dashed lines) are compared with the direct numerical simulation (DNS) of Lee & Reynolds (1985), shown as symbols.

As discussed in Kassinos & Reynolds (1995), the axisymmetric expansion flows exhibit counter-intuitive behavior, where a weaker mean deformation rate produces a level of stress anisotropy $\tilde{r}_{ij}$ that exceeds the one produced under RDT. This effect, which is also supported by the experiments of Choi (1983), is triggered by

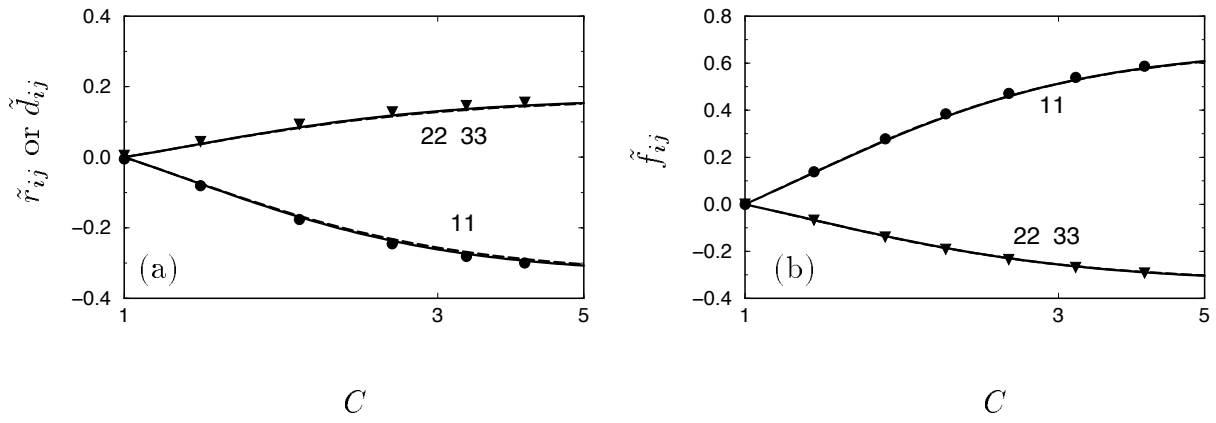

FIGURE 2. Comparison of the one-point model predictions (dashed lines) with the IPRM results (solid lines) and the 1985 DNS of Lee & Reynolds (symbols) for axisymmetric expansion case AXM ($Sq_0^2/\epsilon_0 = 110.0$). (a) evolution of the Reynolds stress and dimensionality anisotropies and (b) evolution of the circulicity anisotropy; 11 component (•), 22 and 33 components (▼).

the different rates of return to isotropy in the **r** and **d** equations, but it is dynamically controlled by the rapid terms. The net effect is a growth of $\tilde{r}_{ij}$ in expense of $\tilde{d}_{ij}$, which is strongly suppressed. As shown in Fig. 2, the predictions of the IPRM and one-point models are almost indistinguishable from each other, and both are able to capture these intriguing effects quite accurately. The predictions of both models for the evolution of the normalized turbulent kinetic energy and dissipation rate are also in good agreement with the DNS.

The case of irrotational axisymmetric expansion flow with rapid strain ($Sq_0^2/\epsilon_0 = 82.0$) is considered in Fig. 4. The agreement between the predictions of the IPRM (solid lines) and those of the one-point (dashed lines) with the simulation results (symbols) is excellent. Also note the drastic difference in the anisotropy evolution histories for $\tilde{r}_{ij}$ and $\tilde{d}_{ij}$ between the slow case (Fig. 3) and the rapid case (Fig. 4) and how these effects are captured by both models.

Plane Strain

A third case of irrotational deformation is considered in Fig. 5, where we show results for initially isotropic homogeneous turbulence subjected to plane strain. The mean deformation is in the x_2-x_3 plane according to

$$S_{ij} = \begin{pmatrix} 0 & 0 & 0 \\ 0 & -S & 0 \\ 0 & 0 & S \end{pmatrix} . \tag{36}$$

Fig. 5 shows evolution histories for the three tensor anisotropies, and for k and ϵ, for a case of weak irrotational plane strain ($Sq_0^2/\epsilon_0 = 1.0$). Again, the IPRM predictions are shown as solid lines and those of the one-point model as dashed

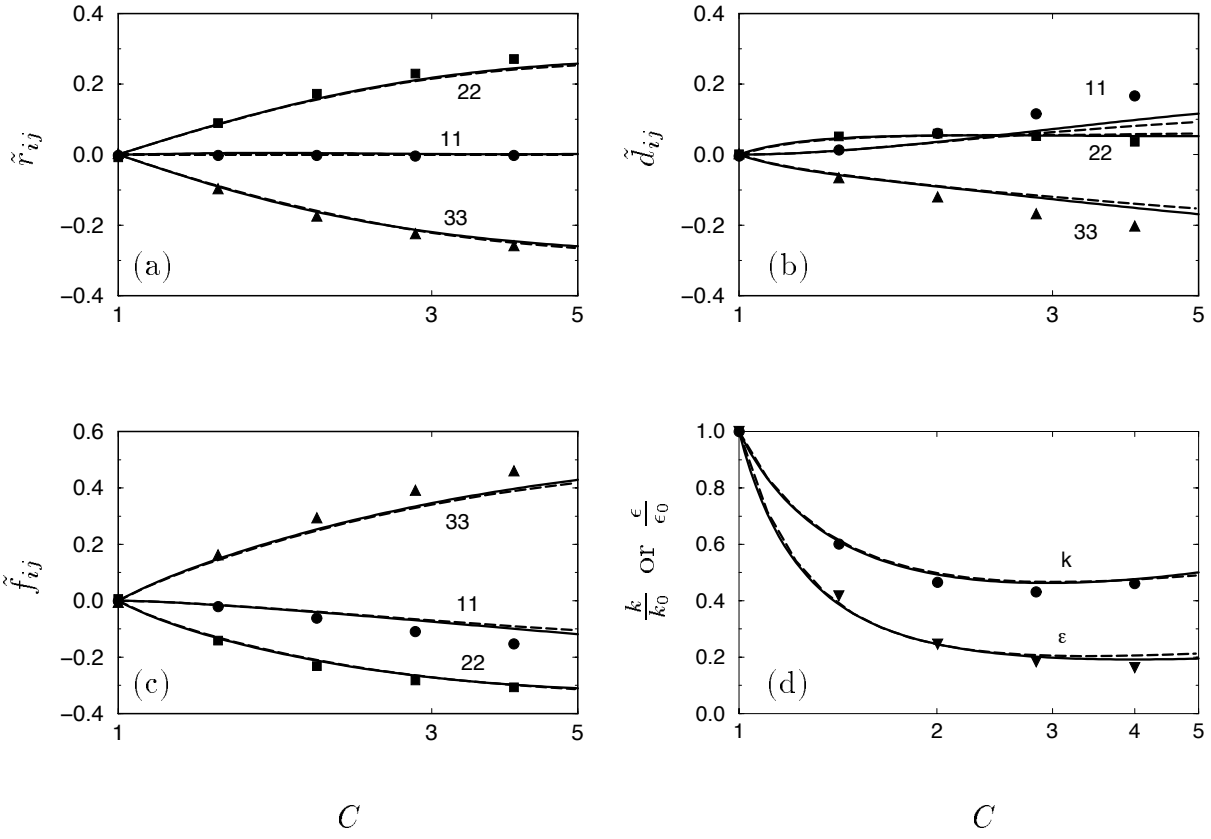

FIGURE 3. Comparison of the one-point model predictions (dashed lines) with the IPRM results (solid lines) and the 1985 DNS of Lee & Reynolds (symbols) for axisymmetric expansion case EXO ($Sq_0^2/\epsilon_0 = 0.82$). (a)-(c) evolution of the the Reynolds stress, dimensionality, and circulicity anisotropies; 11 component (•), 22 and 33 components (▼). (d) evolution of the normalized turbulent kinetic energy (•) and dissipation rate (▼).

lines. Comparison is made with the 1985 DNS of Lee & Reynolds (symbols). Note how the predictions of the one-point model are practically indistinguishable from those of the IPRM and how both models are in excellent agreement with the DNS results for all predictions.

The case of homogeneous, initially isotropic turbulence subjected to rapid irrotational plane ($Sq_0^2/\epsilon_0 = 154.0$) is shown in Fig. 6. Comparison is made with case PXF from the DNS of Lee & Reynolds (1985). Both models are in excellent agreement with the simulation results (symbols). A comparison of the rapid plane strain case (Fig. 6) to the slow plane strain case (Fig. 5) shows that, as in the axisymmetric expansion flow, the rate of straining has a strong effect in the evolution of $\tilde{r}_{ij}$ and $\tilde{d}_{ij}$, and the models are able to capture this.

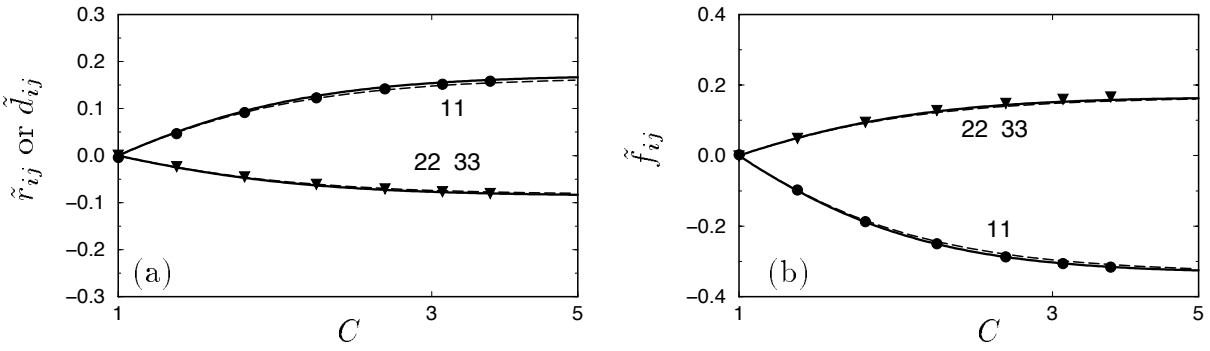

FIGURE 4. Comparison of the one-point model predictions (dashed lines) with the IPRM results (solid lines) and the 1985 DNS of Lee & Reynolds (symbols) for axisymmetric expansion case EXQ ($Sq_0^2/\epsilon_0 = 82$). (a) evolution of the Reynolds stress and dimensionality anisotropies, (b) evolution of the circulicity anisotropy; 11 component (•), 22 and 33 components (▼).

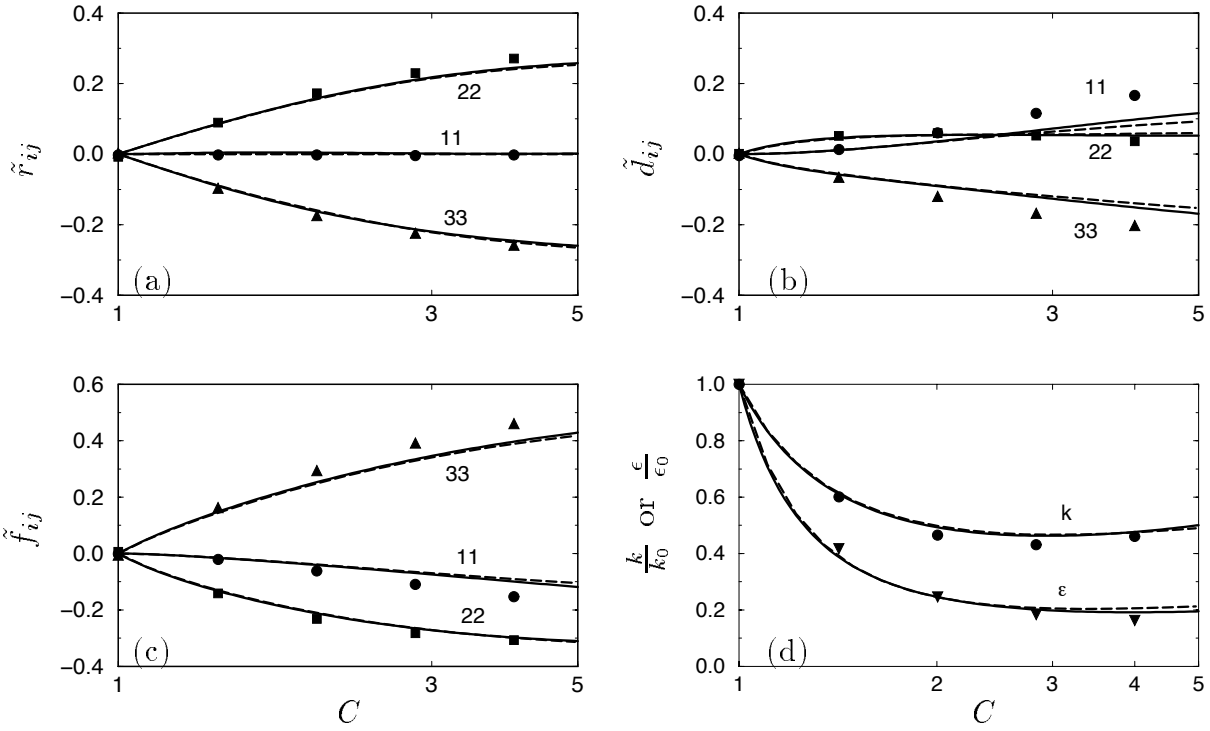

FIGURE 5. Comparison of the one-point model predictions (dashed lines) with the IPRM results (solid lines) and the 1985 DNS of Lee & Reynolds (symbols) for plane strain case PXA ($Sq_0^2/\epsilon_0 = 1.0$). (a)-(c) evolution of the the Reynolds stress, dimensionality, and circulicity anisotropies; 11 component (•), 22 component (■), and 33 component (▼). (d) evolution of the normalized turbulent kinetic energy (•) and dissipation rate (▼).

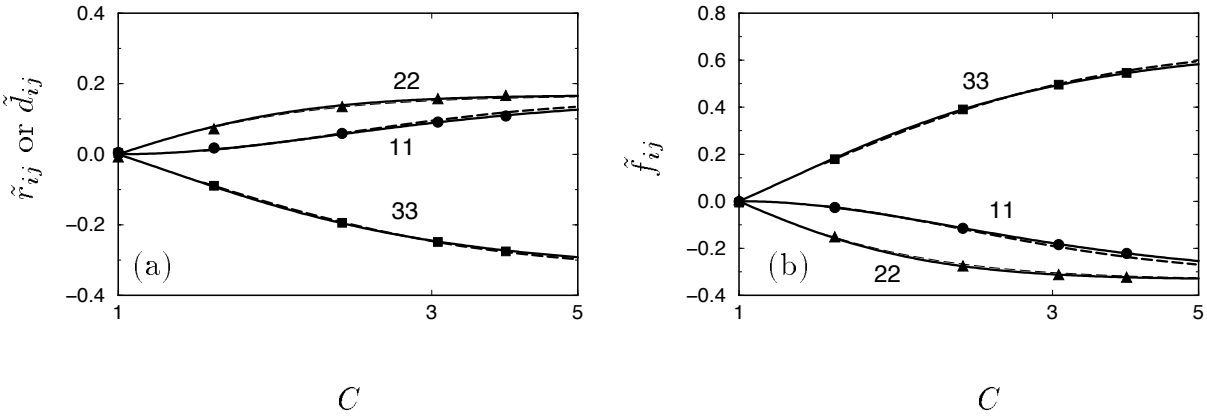

FIGURE 6. Comparison of the one-point model predictions (dashed lines) with the IPRM results (solid lines) and the 1985 DNS of Lee & Reynolds (symbols) for plane strain case PXA ($Sq_0^2/\epsilon_0 = 154.0$). (a) evolution of the Reynolds stress and dimensionality anisotropies, (b) evolution of the circulicity anisotropy 11 component (•), 22 component (■), and 33 component (▼).

3. Remaining issues and future plans

The decomposition given in (28) is valid only under irrotational mean deformations. Under more general modes of deformation, which include combinations of mean strain and mean rotation, reflectional symmetry is broken and stropholysis effects must be included in (28). The exact form of this decomposition under these more general conditions is given by

$$\begin{aligned} M_{ijpq} = {} & \tfrac{1}{2}(Z^f_{ijpq} - Z^r_{ijpq} - Z^d_{ijpq}) + \frac{1}{2}[\epsilon_{zpj}Q^*_{ziq} - \epsilon_{ziq}Q^*_{zpj}] \\ & + \frac{1}{6}\big[-3\delta_{ij}\delta_{pq}q^2 + 4(\delta_{pq}R_{ij} + \delta_{ij}D_{pq}) + 2(\delta_{pq}D_{ij} + \delta_{ij}R_{pq})\big]\,. \end{aligned} \tag{37}$$

The stropholysis Q^*_{ijk} is defined by (see Kassinos & Reynolds 1994)

$$Q_{ijk} = \tfrac{1}{6}[Q_{ijk} + Q_{jki} + Q_{kij} + Q_{ikj} + Q_{jik} + Q_{kji}] \tag{38}$$

where

$$Q_{ijk} \equiv \overline{-u'_j \Psi'_{i,k}}\,. \tag{39}$$

The IPRM representation of Q_{ijk} is given by

$$Q_{ijk} = \langle V^2 s_i v_j n_k \rangle\,. \tag{40}$$

A stropholysis model must satisfy some important constraints. The obvious ones are the requirements that Q^*_{ijk} vanishes under the contraction of any two of its indices, that it is fully symmetric, and that it vanishes whenever any two of the three vectors in the basic triad (**v**, **n**, **s**) are randomly distributed around the third (for example,

in irrotational deformations). In addition, when any of the three tensors $\mathbf{r}$, $\mathbf{d}$, or $\mathbf{f}$ is two-component (2C), the stropholysis must reduce to a special form (see Kassinos & Reynolds 1994). This last of the three constraints is the most challenging to satisfy. What complicates the issue of stropholysis modeling is the fact that whenever any of the three tensors becomes 2C, the three energy-weighted fourth moments (Z^r_{ijpq}, Z^d_{ijpq}, and Z^f_{ijpq}) must also reduce to special forms. To maintain realizability the $\mathbf{Z}$ models must not only reduce to the correct 2C forms, they must also do so at the correct rate in conjunction with the $\mathbf{Q}^*$ model. It seems then that the stropholysis and fourth-moment models cannot be constructed completely independently from each other. This fact is the single most complicating issue in the context of an **R-D** model.

We are currently focusing on the construction of a consistent $\mathbf{Z}$ and $\mathbf{Q}^*$ models that will allow closure of the one-point **R -D** model for the general case, while maintaining full realizability. At the same time we are investigating extensions of the IPRM and one-point models for inhomogeneous flows.

REFERENCES

Bardina, J, Ferziger, J. H., & Reynolds, W. C. 1983 *Improved turbulence models based on large eddy simulation of homogeneous, incompressible, turbulent flows.* Report TF-19, Thermosciences Division, Department of Mechanical Engineering, Stanford University.

Choi, Kwing-So. 1983 *A study of the return to isotropy of homogeneous turbulence*, Technical Report, Sibley school of Mechanical and Aerospace Engineering, Cornell University, New York.

Kassinos, S. C. and Reynolds, W. C. 1994 *A structure-based model for the rapid distortion of homogeneous turbulence.* Report TF-61, Thermosciences Division, Department of Mechanical Engineering, Stanford University.

Kassinos, S. C. and Reynolds, W. C. 1995 An extended structure-based model based on a stochastic eddy-axis evolution equation. *Annual Research Briefs 1995*, Center for Turbulence Research, NASA Ames/Stanford Univ. 133-148.

Kassinos, S. C. and Reynolds, W. C. 1996 An Interacting Particle Representation Model for the Deformation of Homogeneous Turbulence. *Annual Research Briefs 1996*, Center for Turbulence Research, NASA Ames/Stanford Univ. 31-53.

Reynolds, W. C. and Kassinos, S. C. 1995 A one-point model for the evolution of the Reynolds stress and structure tensors in rapidly deformed homogeneous turbulence. *Proc. Roy. Soc. London A.* **451**(1941), 87-104.

Lee, M. J. & Reynolds, W. C. 1985 *Numerical experiments on the structure of homogeneous turbulence".* Report TF-24, Thermosciences Division, Department of Mechanical Engineering, Stanford University.

MANSOUR, N. N., SHIH, T.-H., & REYNOLDS, W. C. 1991 The effects of rotation on initially anisotropic homogeneous flows. *Phys. Fluids A.* **3,** 2421–2425.

POPE, S. B. 1994 On the relationship between stochastic Lagrangian models of turbulence and second-moment closures. *Phys. Fluids.* **6,** 973–985.

SPEZIALE, C. G. 1981 Some interesting properties of two-dimensional turbulence. *Phys. Fluids.* **24**(8), 1425-1427.

SPEZIALE, C. G. 1985 Modeling the pressure-velocity correlation of turbulence. *Phys. Fluids.* **28**(8), 69-71.

VANSLOOTEN, P. R. & POPE, S. B. 1997 Pdf modeling for inhomogeneous turbulence with exact representation of rapid distortions. *Phys. Fluids.* **9**(4), 1085-1105.